X-ray scattering with momentum transfer in the plane of membrane
Application to gramicidin organization

Ke He, Steven J. Ludtke, Yili Wu, and Huey W. Huang

Physics Department, Rice University, Houston, Texas 77251-1892 USA

ABSTRACT   We demonstrate a technique for measuring x-ray (or neutron) scattering with the momentum transfer confined in the plane of membrane, for the purpose of studying lateral organization of proteins and peptides in membrane. Unlike freeze-fracture electron microscopy or atomic force microscopy which requires the membrane to be frozen or fixed, in-plane x-ray scattering can be performed with the membrane maintained in the liquid crystalline state. As an example, the controversial question of whether gramicidin forms aggregates in membrane was investigated. We used dilauroylphosphatidylcholine (DLPC) bilayers containing gramicidin in the molar ratio of 10:1. Very clear scattering curves reflecting gramicidin channel-channel correlation were obtained, even for the sample containing no heavy atoms. Thallium ions bound to gramicidin channels merely increase the magnitude of the scattering curve. Analysis of the data shows that the channels were randomly distributed in the membrane, similar to a computer simulation of freely moving disks in a plane. We suggest that oriented proteins may provide substantial x-ray contrast against the lipid background without requiring heavy-atom labeling. This should open up many possible new experiments.

INTRODUCTION

We report a successful measurement of x-ray scattering with the momentum transfer confined in the plane of membrane. This technique is ideal for the measurement of the lateral organization of proteins and peptides in membranes. It has long been noted that membrane proteins tend to aggregate, even in the absence of cytoskeletal interactions (Feingold, 1976; Melhorn and Packer, 1976; Copps et al., 1976; Pearson et al., 1979; Lewis and Engelman, 1983; Pearson et al., 1983; Pearson et al., 1984). Amphipathic α-helical peptides are known to form transmembrane ion channels in some unknown oligomeric forms (e.g., alamethicin, Latotte and Alvarez, 1981; melittin, Tosteson and Tosteson, 1981; magainins, Duclohier et al., 1989; synthetic peptides, Oiki et al., 1988; and Lear et al., 1988); there is indication that they also form aggregates on the membrane surface before insertion into membrane (Huang and Wu, 1991). Protein aggregation has been observed by freeze-fracture electron microscopy (Feingold, 1976; Melhorn and Packer, 1976; Copps et al., 1976; Pearson et al., 1979; Lewis and Engelman, 1983; Pearson et al., 1983; Pearson et al., 1984). However the resolution of this technique is not fine enough to detect small peptides. Also, the possibility of artifacts in the freeze-fracture process is difficult to assess (Pearson et al., 1984). Atomic force microscopy is potentially a powerful tool for imaging membrane proteins (Butt et al., 1990; Lacapere et al., 1992). But again, the membrane has to be fixed, otherwise the probing force would move the molecules, making imaging impossible (Lacapere et al., 1992). Thus, the greatest advantage of the scattering method is its applicability to the liquid crystalline (L_α) state of membranes. With suitably labeled samples, in-plane x-ray or neutron scattering provides a direct measurement of the lateral particle-particle correlation in the plane of the membrane.

As an example of in-plane scattering, we investigated the organization of gramicidin in membrane. There have been reports of possible gramicidin organization in membrane (Spisni et al., 1983; Killian and de Kruijff, 1988). Stark et al. (1986) has argued that the conducting channel of gramicidin is a tetramer or a higher oligomer. We used hydrated dilauroylphosphatidylcholine (DLPC) containing gramicidin in the molar ratio of 10:1. This sample has been studied previously by x-ray lamellar diffraction to determine the binding sites for monovalent and divalent cations in the gramicidin channel (Olah et al., 1991; Liu et al., 1991). Gramicidin in this membrane is in the channel form (Huang and Olah, 1987; Olah et al., 1991). Our in-plane scattering result shows that dimeric gramicidin channels distribute randomly in the membrane. Thus, it appears that, at least in DLPC bilayers, gramicidin does not form aggregates.

EXPERIMENTAL

Materials and preparation of samples

The materials and sample preparation were the same as described in Olah et al. (1991). The hydrated mixtures of gramicidin and DLPC with or without thallium acetate (in the lipid/peptide/ion molar ratio 10:1:1 or 10/1/0) were aligned into uniform multilayers between two SiO₂-coated, polished beryllium plates (314 μm × 10 mm dia.). The water-intercalated multiple lipid bilayers were parallel to the substrate surfaces in the form a smectic A liquid crystal. This type of preparation inevitably contains smectic defects (Huang and Olah, 1987). It is important to diminish these defects as much as possible (see below). The thickness of the multilayers was ~20 μm. The sample was housed in a humidity chamber equipped with kapton windows during the x-ray experiment.

X-ray lamellar diffraction (in which the momentum transfer is perpendicular to the planes of the multilayers) of these samples showed that the majority of thallium ions are bound to the dimeric gramicidin channels (Olah et al., 1991). This is consistent with most studies of ion
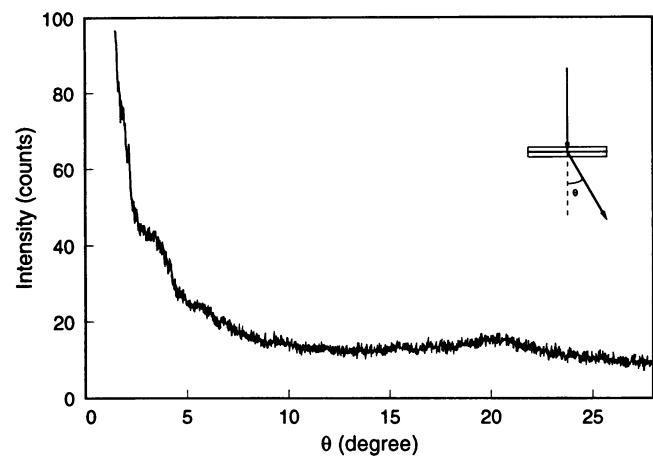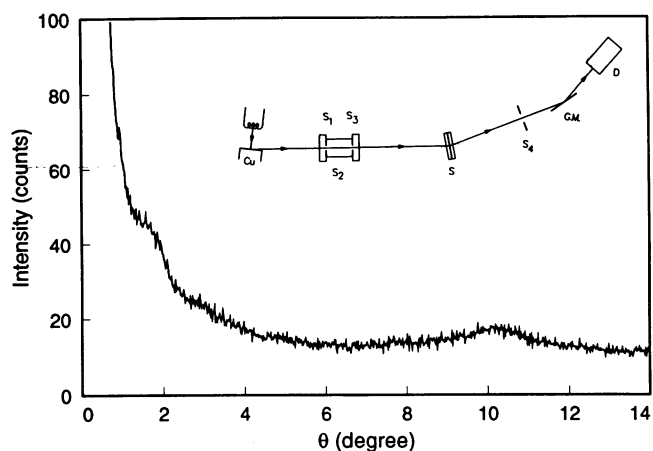
raw data of θ-2θ scan and 0-2θ scan on a gramicidin sample are essentially the same. It is obvious that 0-2θ scan is advantageous if one uses an area detector. At $\sim 1°$ ($2°$ in the 0-2θ scan) one notices a small peak, that is the first Bragg peak of lamellar diffraction (see also Fig. 2). In these measurements the momentum transfer of the photon scattering is parallel to the substrate surfaces; therefore, if the membranes are aligned homeotropically, the results are in-plane scatterings. However, if the sample contains smectic defects where the bilayers may be oriented perpendicular to the substrate surfaces, the results will contain lamellar diffraction. The lamellar diffraction of a multilayer sample is much stronger than the in-plane scattering. For example, if we turn the sample by $90°$ about an axis normal to the plane of the figure, the first-order lamellar diffraction would be typically $\sim 10^4$ counts per second, compared with ~ 70 counts per second for in-plane scattering at the same angle. Thus, the technique for preparing a well aligned multilayer sample (Huang and Olah, 1987) is essential for in-plane measurements. If a sample is not aligned well, that is, if it contains too many defects, the lamellar peaks would swamp the in-plane signal.

Fig. 2 shows the in-plane scattering of membranes containing gramicidin with or without thallium ions and that of pure membrane con-

FIGURE 1 The raw data of in-plane scattering from a gramicidin/ DLPC sample by θ-2θ (top) and 0-2θ (bottom) scans; background has not been subtracted. The inset (top) shows the schematic of the x-ray diffractometer. S_1, S_3, and S_4 are vertical slits; S_2, horizontal soller slits; S, the sample, G.M. a graphite monochromator; and D, a scintillation detector.

adsorption to pure phosphatidylcholine bilayers, where no binding of monovalent cations was found (Lis et al., 1981a; Lis et al., 1981b; Altenbach and Seelig, 1984). (It should also be noted that although the adsorption of divalent cations to phosphatidylcholine bilayers is well known, the binding decreases with the interbilayer separation; and there is no evidence of divalent ion binding for the separations less than 20 Å; see Lis et al., 1981a; Lis et al., 1981b.) Additionally, when samples of gramicidin, thallium acetate (or potassium acetate) and DLPC in the molar ratio of 10:1:1 were prepared, the mixtures readily turned into homogeneous hydrated multilayers; however, the same samples without gramicidin always excluded the salt (the salt precipitated and crystallized). Thus, all evidence indicates that the majority of ions are associated with gramicidin rather than with the lipid head groups.

X-ray in-plane scattering

The experiment was carried out with a line source of copper K_α radiation operating at 40 Kv and 35 mA. The arrangement is shown schematically in Fig. 1. The incident beam is collimated by two vertical slits S_1 and S_3, and by horizontal Soller slits S_2. The detector consists of a vertical slit S_4, a graphite monochromator (G.M.), and a scintillation counter (D) which was biased to discriminate against higher harmonics. In-plane scattering can be carried out by θ-2θ scan or by normal incidence (we call the latter geometry 0-2θ scan). Fig. 1 shows that the
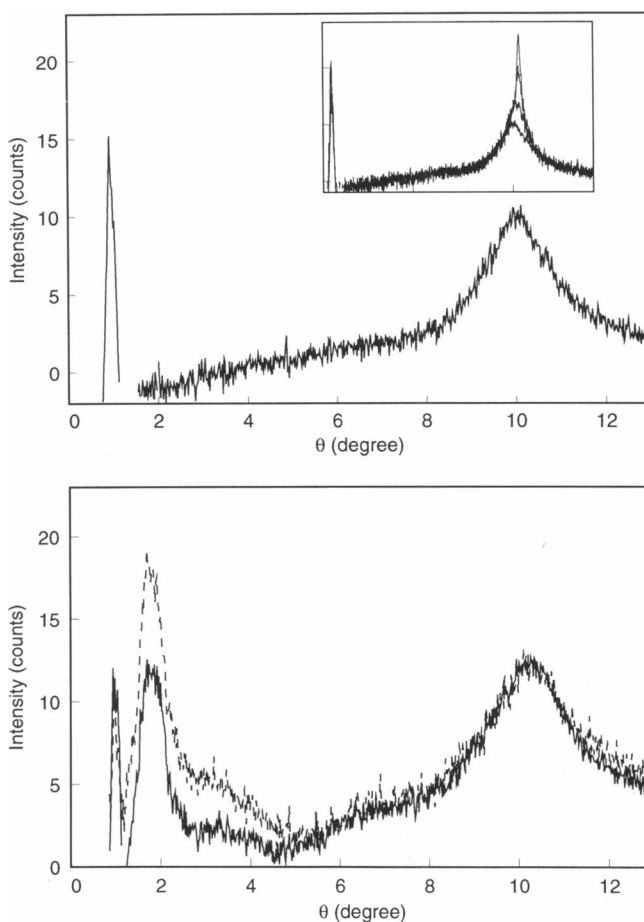

FIGURE 2 (Top) In-plane scattering intensity of pure DLPC bilayers. (Bottom) In-plane scattering intensities of DLPC bilayers containing gramicidin with thallium ions (molar ratio 10:1:1, dashed line) and without thallium (molar ratio 10:1:0, solid line). The samples were equilibrated in 100% RH. The background signal of the beryllium plates and kapton windows has been removed from the data. The inset (top) shows the in-plane scattering intensities of pure DLPC bilayers changing with humidity. The bottom curve was scanned at 100% RH. The other three, the second from the bottom to the top, were scanned, respectively, 10, 20, and 30 h after the sample was exposed to 60% RH.
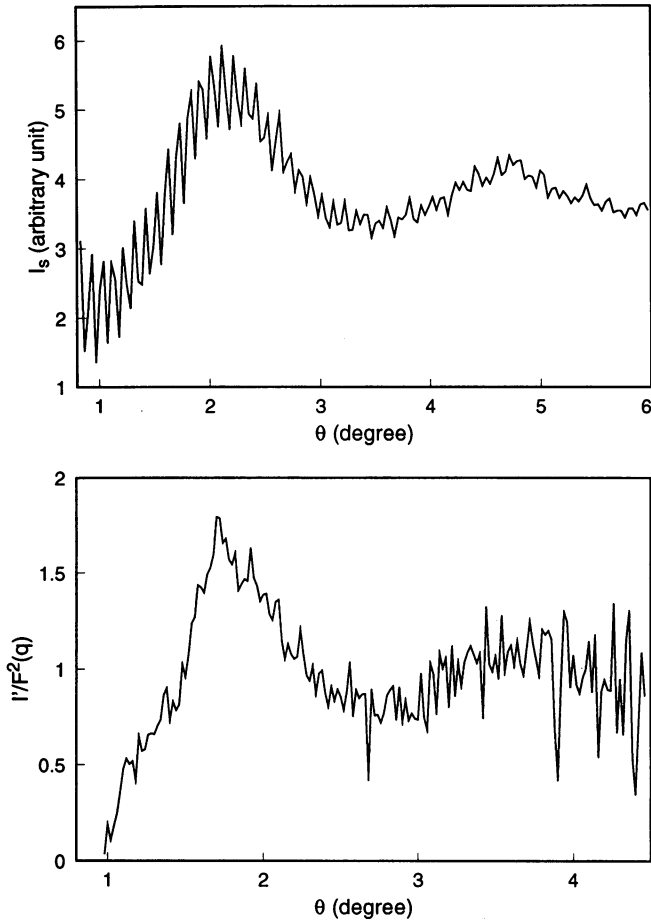
FIGURE 3 (*Top*) The simulated intensity of freely moving disks having the same concentration as the gramicidin in the sample. The intensity does not include the form factor of the disk. (*Bottom*) The scattering intensity of gramicidin (from Fig. 2, *bottom, dashed line*) divided by the square of an assumed form factor $F(q)$ (see Fig. 4, *top*).

taining no gramicidin, after the background signal of beryllium plates and kapton windows was subtracted. Surprisingly, the gramicidin signal without thallium ($<6°$) is very clear. The thallium merely increases the intensity of the gramicidin signal as expected. The scattering curves (not including those in the inset) were all obtained at 100% RH. The inset shows the pure lipid bands at various humidities, the bottom curve at 100% RH and three subsequent curves after the sample was exposed to 60% RH. In high humidity, the diffuse band near 4.5 Å indicates that the lipid is in the liquid crystalline state (Luzatti, 1968; Levine and Wilkins, 1971). In low humidity, the sharp peak near 4.3 Å indicates that the lipid turns into the gel phase (Tardieu et al., 1973; Janiak et al., 1976).

Computer simulation

275 circular disks are randomly distributed on a square plane. The ratio of the area occupied by the disks to the area they are confined in is the same as gramicidin in membrane, $\sim32\%$. The disks are given equal mass and a random initial velocity, and then undergo classical motion. All disk-disk and disk-wall collisions are elastic. The simulated scattering intensity $I_s = |\Sigma_j \exp(i\mathbf{q}\cdot\mathbf{r}_j)|^2$ was computed and averaged over time (Fig. 3, *top*). The form factor of the disk is not included. The ripple on the curve is the artifact due to the finite size of the confinement area.

THEORETICAL ANALYSIS

General

The theory of x-ray scattering is well known (e.g., James, 1948; Warren, 1969). The purpose of this section is to establish the appropriate notations and formulas for data analysis.

The x-ray scattering intensity I is given by

$$I/I_e = \sum_m \sum_n f_m(q)f_n(q) \exp[i\mathbf{q}\cdot(\mathbf{r}_m - \mathbf{r}_n)], \quad (1)$$

where $I_e = \text{const}\cdot(1 + \cos^2 2\theta \cos^2 2\theta_M)$ is the scattering intensity by a single free electron, $\theta_M = 13.28°$ is the Bragg angle of the graphite monochromator, $f_m(q)$ is the scattering form factor of atom m at the position $\mathbf{r}$, and $\mathbf{q}$ is the momentum transfer of elastic scattering with magnitude q equal to $4\pi \sin \theta/\lambda$. It has been known since the 1960's that the hydrocarbon chains of bilayer membranes in the liquid crystalline state produce a single broad band at $q = 2\pi/(4.6 \text{ Å})$. This has been recognized to be of the same origin as the diffraction peak of liquid paraffins, irrespective of the number of carbon atoms in the chain (Luzatti, 1968; Levine and Wilkins, 1971; Warren, 1933). Outside of this liquid-paraffin peak, the in-plane scattering curve of a pure lipid is flat and featureless (see Fig. 2). The first step of data analysis is to separate the lipid signal from the rest.

For this purpose, it is more convenient to convert the summations in Eq. 1 to integrals by introducing a scattering density function $\rho(\mathbf{r})$ such that $\rho(\mathbf{r})dV(\mathbf{r})$ is the number of atoms, each multiplied by its form factor, in the volume element $dV(\mathbf{r})$ at the position $\mathbf{r}$

$$I/I_e = \int\int \rho(\mathbf{r})\rho(\mathbf{r}') \exp[i\mathbf{q}\cdot(\mathbf{r}' - \mathbf{r})] \, dV(\mathbf{r}) \, dV(\mathbf{r}'). \quad (2)$$

Let us separate the space of integration into two: $\int = \int_p + \int_l$, where $\int_p$ integrates over the space occupied by the protein molecules and $\int_l$ over the space occupied by the lipid molecules. Let ρ_p be the scattering density of the protein molecules and ρ_l that of the lipid molecules. It is easy to show that Eq. 2 can be written as

$$I/I_e = \Big\{ \int\int \rho_l(\mathbf{r})\rho_l(\mathbf{r}') + \int_p \int [\rho_p(\mathbf{r}) - \rho_l(\mathbf{r})]\rho_l(\mathbf{r}')$$

$$+ \int \int_p \rho_l(\mathbf{r})[\rho_p(\mathbf{r}') - \rho_l(\mathbf{r}')]$$

$$+ \int_p \int_p [\rho_p(\mathbf{r}) - \rho_l(\mathbf{r})][\rho_p(\mathbf{r}') - \rho_l(\mathbf{r}')]\Big\}$$

$$\times \exp[i\mathbf{q}\cdot(\mathbf{r}' - \mathbf{r})] \, dV(\mathbf{r}) \, dV(\mathbf{r}'), \quad (3)$$

where $\int_p \rho_l \, dV$ implies that the space occupied by the protein molecules is replaced by the lipid molecules. The first term represents the scattering intensity by a pure lipid membrane. The second and the third terms contain the scattering intensity of a single protein molecule em-

bedded in an otherwise pure lipid membrane. Unless diffraction peaks corresponding to such correlations are present in the data, we will be concerned only with the correlations among protein molecules, that is the last term of Eq. 3,

$$I'/I_e = \int_p \int_p [\rho_p(\mathbf{r}) - \rho_1(\mathbf{r})][\rho_p(\mathbf{r}') - \rho_1(\mathbf{r}')]$$
$$\times \exp[i\mathbf{q}\cdot(\mathbf{r}' - \mathbf{r})]\, dV(\mathbf{r})\, dV(\mathbf{r}'). \quad (4)$$

For simplicity, we consider a membrane containing only one kind of protein. Define the effective molecular form factor for a protein as follows,

$$F(q) = \int [\rho_p(\mathbf{r}) - \rho_1(\mathbf{r})] \exp[i\mathbf{q}\cdot(\mathbf{r} - \mathbf{r}_a)]\, dV(\mathbf{r}), \quad (5)$$

where $\mathbf{r}_a$ is the position of the molecular axis and the integration is over the space occupied by the protein. Let us assume that the protein is cylindrically symmetric with respect to the molecular axis which is in the z direction, perpendicular to the plane of the membrane (the xy plane). Then the form factor F is a real function of the magnitude of $\mathbf{q}$, as indicated in Eq. 5. Then Eq. 4 becomes

$$I'/I_e = \sum_a F^2(q) + \sum_a F^2(q) \sum_{b \neq a} \exp[i\mathbf{q}\cdot(\mathbf{r}_b - \mathbf{r}_a)]. \quad (6)$$

Consider a bilayer of area A, containing N number of protein molecules. Since $\mathbf{q}$ is confined in the xy plane, only the in-plane component of $\mathbf{r}$ is relevant; so from now on we will regard $\mathbf{r}$ to be representing the position of a protein in the plane of membrane. Let $n(\mathbf{r})d\sigma$ be the number of molecular axes in the area element $d\sigma$ at a position $\mathbf{r}$ relative to a protein, averaged over the sample. In the liquid crystalline state, $n(\mathbf{r})$ has cylindrical symmetry; it can be written as $n(r)$. In converting the last summation in Eq. 6 to an integral, it is useful to add and subtract a term involving $\bar{n}\,(=N/A)$, so that we have

$$I'/I_e = NF^2(q) + NF^2(q) \int [n(r) - \bar{n}]J_0(qr)2\pi r\, dr$$
$$+ NF^2(q)\bar{n} \int J_0(qr)2\pi r\, dr, \quad (7)$$

where $J_0(qr)$ is the zeroth order Bessel function. The last integral is essentially confined within a small angle $q \leq 2\pi/L$. L is the linear size of the sample in the xy plane, a few millimeters in this case; that makes the integral insignificant for $\theta > 1$ millidegree. Therefore, it is negligible. On the other hand, the integral in the second term usually extends only over a short range, because $n(r) - \bar{n}$ approaches zero for r greater than a few interprotein distances if the sample is in the liquid state. Although the experimental intensity is usually obtained in arbitrary units, there are ways to put I'/NI_e in absolute units if we know the form factor $F(q)$ (Warren, 1969). The radial

distribution function $2\pi r n(r)$ can then be evaluated by the Bessel transform (Watson, 1966),

$$2\pi r n(r) = 2\pi r\bar{n} + r \int \{I'/[NI_e F^2(q)] - 1\}J_0(qr)q\, dq. \quad (8)$$

Gramicidin in membrane

The cross section of the DLPC molecule in the L_α phase is ~52 Å^2 (Olah et al., 1991; Small, 1986). In crystals (grown from organic solvents) the volume of a gramicidin dimer is 6,192 Å^3 without ions (Langs, 1988) and 6518 Å^3 with CsCl (Wallace and Ravikumar, 1988). The dimers in these crystals are not the channel form. But we will assume that the molecular volume of the dimeric channel is more or less the same as those of the crystalline dimers, in order to estimate the channel cross section. From the symmetric binding sites of divalent cations at the mouths of the channel (Olah et al., 1991), we know that the length of the channel is ~26 Å. Thus, we estimate the cross section of the gramicidin channel to be ~250 Å^2, corresponding to a 9 Å radius. If we uniformly distribute the gramicidin in DLPC bilayer in the molar ratio 1/10, the average distance between the neighboring gramicidin channels is 30 Å.

The scattering data concerning gramicidin organization are contained in $1° < \theta < 5°$. The prominent peak at $1.7°$ corresponds to the first maximum of $J_0(qr)$ at $qr = 7.016$ (see Eqs. 7 and 8). Thus, the position of this peak alone gives us the correlation distance of gramicidin to be ~29 Å. The scattering data are qualitatively similar to the simulated intensity curve, indicating that the nature of the particle distribution in the sample is qualitatively similar to that in the simulation (that is, the distribution of gramicidin is essentially random). However, the simulated result has its first peak at a higher angle, indicating a closer correlation distance of ~24 Å, and it has a relatively larger second peak. There are at least three factors that may contribute to these discrepancies. First, if we include the molecular form factor in the simulated intensity its peak positions would shift slightly to smaller angles and its second peak would be significantly reduced (see below). Second, there are uncertainties in the molecular cross sections and in the lipid/peptide molar ratio in the sample. Third, we expect the presence of lipid molecules to somewhat influence the distribution of gramicidin.

More detailed analyses require some knowledge about the form factor $F(q)$. We note that all atomic form factors are relatively constant in the region of interest ($<4°$), decreasing from 1.0 (times the atomic number) at $\theta = 0°$ to about ≥ 0.95 at $\theta = 5°$. Therefore, the important q-dependence of $F(q)$ comes from the size and, to a lesser degree, the shape of the gramicidin channel. Only the rigid part of the molecule will contribute to the form factor. If the backbone of the gramicidin channel is the main contributor to the form factor, the q-dependence may be estimated by using a cylindrical shell of inner
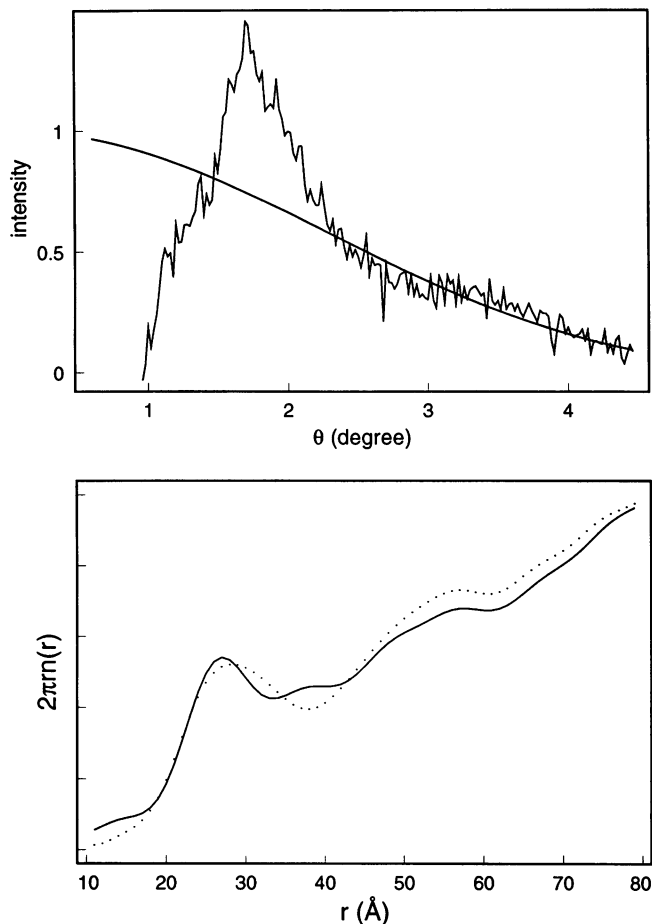
FIGURE 4   (*Top*) A hypothetical form factor for the gramicidin backbone in the channel form, normalized to one at $\theta = 0°$. The scattering intensity of gramicidin (from Fig. 2, *bottom, dashed line*) is multiplied by a constant factor to match the form factor at the high angle region. (*Bottom*) The radial distribution function $2\pi r n(r)$, unnormalized, if we use the form factor (*solid line*) and if we ignore the form factor (*dotted line*).

diameter equal to 4 Å and outer diameter 18 Å. Its q-dependence is shown in Fig. 4 (*top*). The intensity (Fig. 2, *dashed line*) divided by the square of this q-dependence is shown in Fig. 3 (*bottom*) to be compared with the simulated intensity (Fig. 3, *top*). If we use this $I'/F^2(q)$ (i.e., Fig. 3, *bottom*) in Eq. 8, we obtain an unnormalized radial distribution function $2\pi r n(r)$ (Fig. 4, *bottom*). The radial distribution obtained by ignoring the form factor is also shown for comparison. The maxima of these radial distribution functions are at 27 and 28 Å, respectively. It is clear from these analyses that gramicidin channels in a DLPC bilayer are randomly distributed; at the molar ratio of 1 to 10, the correlation distance between channels is ~28 Å.

DISCUSSION

In an earlier paper (Huang, 1986), we studied the elastic property of a bilayer membrane and its effect on the

lifetime of gramicidin channels. We speculated that if the hydrophobic thicknesses of the bilayer and the channel mismatch, there will be a membrane-mediated attractive force between neighboring channels. This possible effect may be very weak here, because the lifetime of a gramicidin channel is near maximum in a membrane of thickness approximate that of DLPC (Huang, 1986), perhaps, indicating that the hydrophobic thicknesses of the bilayer and the channel are about the same. If this is the case, our result implies that gramicidin channels do not aggregate by themselves (in the absence of possible lipid-mediated forces). Whether they would aggregate in a thicker membrane remains to be investigated.

Perhaps the most surprising and important result of this experiment is that the protein signal stands out clearly against the lipid background without the benefit of heavy atoms (Fig. 2). Normally, the average bulk electron density of protein (0.33 $e/\text{Å}^3$ in the case of gramicidin) is close to that of lipid (0.35 $e/\text{Å}^3$ in the case of DLPC). And one does not expect to see protein signal by x-ray scattering without heavy-atom labeling. For this reason, neutron scattering with deuterated samples is often preferred for studying protein correlations. The difference here is that the protein molecules are oriented in the membrane and the in-plane scattering depends on the areal electron density rather than the bulk electron density. If a protein is oriented, there may be areas of high and low electron densities in different parts of the cross section. For example the cylindrical shell of the gramicidin backbone discussed earlier has an areal electron density in the xy plane about twice that of the lipid background. This discovery, that protein signal can be detected in membrane without labeling, should open up many possible new experiments.

REFERENCES

Altenbach, C., and J. Seelig. 1984. Ca²⁺ binding to phosphatidylcholine bilayer as studied by deuterium magnetic resonance. Evidence for the formation of a Ca²⁺ complex with two phospholipid molecules. *Biochemistry.* 23:3913–3920.

Butt, H.-J., D. H. Downing, and P. K. Hansma. 1990. Imaging the membrane protein bacteriorhodopsin with atomic force microscope. *Biophys. J.* 58:1473–1480.

Copps, T. P., W. S. Chelack, and A. Petkau. 1976. Variation in distribution of membrane particles in *Acholeplasma laidlawii* B with pH. *J. Ultrastruct. Res.* 55:1–3.

Duclohier, H., G. Molle, and G. Spach. 1989. Antimicrobial peptide magainin 1 form *Xenopus* sken forms anion-permeable channels in planar lipid bilayers. *Biophys. J.* 56:1017–1021.

Feingold, L. 1976. Cell membrane fluidity: molecular modeling of par-

ticle aggregations seen in electron microscopy. *Biochim. Biophys. Acta.* 448:393-398.

Huang, H. W. 1986. Deformation free energy of bilayer membrane and its effect on gramicidin channel lifetime. *Biophys. J.* 50:1061-1070.

Huang, H. W., and G. A. Olah. 1987. Uniformly oriented gramicidin channels embedded in thick monodomain lecithin multilayers. *Biophys. J.* 51:989-992.

Huang, H. W., and Y. Wu. 1991. Lipid-alamethicin interactions influence alamethicin orientation. *Biophys. J.* 60:1079-1087.

Huang, H. W., W. Liu, G. A. Olah, and Y. Wu. 1991. Physical techniques of membrane studies: study of membrane active peptides in bilayers. *Prog. Surface Sci.* 38:145-199.

James, R. W. 1948. The optical principles of the diffraction of x-rays. Ox Bow Press, Woodbridge, CT. 458-512

Janiak, M. J., D. M. Small, and G. G. Shipley. 1976. Nature of the thermal pretransition of synthetic phospholipids: dimyristoyl- and dipalmitoyllecithin. *Biochemistry.* 15:4575-4580.

Killian, J. A., and B. de Kruijff. 1988. Proposed mechanism for H_{II} phase induction by gramicidin in model membranes and its relation to channel formation. *Biophys. J.* 53:111-117.

Lacapere, J.-J., D. Stokes, and D. Chatenay. 1992. Atomic force microscopy of three-dimensional membrane protein crystals. *Biophys. J.* 63:303-308.

Latorre, R., and O. Alvarez. 1981. Voltage-dependent channels in planar lipid bilayer membranes. *Physiol. Rev.* 61:77-150.

Lang, D. A. 1988. Three-dimensional structure at 86 Å of the uncomplexed form of the transmembrane ion channel peptide gramicidin A. *Science (Wash. DC).* 241:188-191.

Lear, J. D., Z. R. Wasserman, and W. F. Degrado. 1988. Synthetic amphiphilic peptide models for protein ion channels. *Science (Wash. DC).* 240:1177-1181.

Levine, Y. K., and M. H. F. Wilkins. 1971. Structure of oriented lipid bilayers. *Nature (Lond.).* 230:69-72.

Lewis, B. A., and D. M. Engelman. 1983. Bacteriorhodopsin remains dispersed in fluid phospholipid bilayers over a wide range of bilayer thicknesses. *J. Mol. Biol.* 166:203-210.

Lis, L. J., V. A. Parsegian, and R. P. Rand. 1981. Binding of divalent cations to dipalmitoylphosphatidylcholin bilayers and its effect on bilayer interaction. *Biochemistry.* 20:1761-1770.

Lis, L. J., W. T. Lis, V. A. Parsegian, and R. P. Rand. 1981. Adsorption of divalent cations to a variety of phosphatidylcholine bilayers. *Biochemistry.* 20:1771-1777.

Liu, W., T. Y. Teng, Y. Wu, and H. W. Huang. 1991. Phase determination for membrane diffraction by anomalous dispersion. *Acta Cryst.* A47:553-559.

Luzzati, V. 1968. X-ray diffraction studies of lipid-water systems. *In* Biological Membranes. D. Chapman, editor. Academic Press, New York. 71-124

Melhorn, J., and L. Packer. 1976. Analysis of freeze-fracture electron micrographs by a computer-based technique. *Biophys. J.* 16:613-625.

Oiki, S., W. Danho, V. Madison, and M. Mantal. 1988. M2δ, a candidate for the structure lining the ionic channel of the nicotinic cholinergic receptor. *Proc. Natl. Acad. Sci. USA.* 85:8703-8707.

Olah, G. A., H. W. Huang, W. Liu, and Y. Wu. 1991. Location of ion binding sites in the gramicidin channel by x-ray diffraction. *J. Mol. Biol.* 218:847-858.

Pearson, R. P., S. W. Hui, and T. P. Stewart. 1979. Correlative statistical analysis and computer modeling of intramembranous particle distributions in human erythrocyte membranes. *Biochim. Biophys. Acta.* 557:265-282.

Pearson, L. T., S. I. Chan, B. A. Lewis, and D. M. Engelman. 1983. Pair distribution functions of bacteriorhodopsin and rhodopsin in model bilayers. *Biophys. J.* 43:167-174.

Pearson, L. T., J. Edelman, and S. I. Chan. 1984. Statistical mechanics of lipid membranes. Protein correlation functions and lipid ordering. *Biophys. J.* 45:863-871.

Small, D. M. 1986. The Physical Chemistry of Lipids. Plenum Press, New York. 475-522.

Spisni, A., I. Pasquali-Ronchetti, Casali, E., L. Lindner, P. Cavatorta, L. Masotti, and D. W. Urry. 1983. Supramolecular organization of lysophosphatidylcholine packaged gramicidin A'. *Biochim. Biophys. Acta.* 732:58-68.

Stark, G., M. Strässle, and Z. Takacz. 1986. Temperature-jump and voltage-jump experiments at planar lipid membranes support an aggregational (micellar) model of the gramicidin A ion channel. *J. Membr. Biol.* 89:23-37.

Tardieu, A., V. Luzzati, and F. C. Reman. 1973. Structure and polymorphism of hydrocarbon chains of lipids: a study of lecithin-water phases. *J. Mol. Biol.* 75:11-733.

Tosteson, M. T., and D. C. Tosteson. 1981. The sting: melittin forms channels in lipid bilayers. *Biophys. J.* 36:109-116.

Wallace, B. A., and K. Ravikumar. 1988. The gramicidin pore: crystal structure of a cesium complex. *Science (Wash. DC).* 241:182-187.

Warren, B. E. 1933. X-ray diffraction in long chain liquids. *Phys. Rev.* 44:969-973.

Warren, B. E. 1969. X-ray Diffraction. Dover, New York. 116-150.

Watson, G. N. 1966. Theory of Bessel Functions. Cambridge University Press, New York. 453 pp.